Metadata of the chapter that will be visualized online

Chapter Title	Effect of Strain Softening Behaviours on Run-Out Distance of a Sensitive Clay Landslide	
Copyright Year	2017	
Copyright Holder	Springer International Publishing AG	
Corresponding Author	Family Name	**Fornes**
	Particle	
	Given Name	**Petter**
	Suffix	
	Organization	Norwegian Geotechnical Institute (NGI)
	Address	Oslo, Norway
	Organization	Norwegian University of Science and Technology (NTNU)
	Address	Trondheim, Norway
	Email	pfo@ngi.no
Author	Family Name	**Khoa**
	Particle	
	Given Name	**Huynh D. V.**
	Suffix	
	Organization	Norwegian Geotechnical Institute (NGI)
	Address	Oslo, Norway
Abstract	Reliable prediction of landslide triggering threshold and landslide run-out distance is essential for hazard risk assessment. The paper focuses on studying slides in sensitive clays, which represent a major geohazard in many countries including Norway, Sweden and eastern Canada. Large deformation finite element (FE) analyses were performed using the Coupled Eulerian-Lagrangian (CEL) method in Abaqus, which allows for capturing of the full progressive failure mechanism (initiation, propagation and breakoff) involved in a sensitive clay slide. The 1984 slide in Vestfossen, Norway, was chosen as problem case of progressive failure in sensitive clay to be back-calculated by using the CEL FE-model. It is found that the failure mechanism predicted by the FE-analysis agrees reasonably well with the historical failure mode observed at Vestfossen. A parametric study has been performed on the remoulded shear strength as well as the rate of strain softening of the sensitive clay in order to evaluate their effects on the landslide run-out distance.	

Chapter 31
Effect of Strain Softening Behaviours on Run-Out Distance of a Sensitive Clay Landslide

AQ1

Petter Fornes and Huynh D. V. Khoa

Abstract Reliable prediction of landslide triggering threshold and landslide run-out distance is essential for hazard risk assessment. The paper focuses on studying slides in sensitive clays, which represent a major geohazard in many countries including Norway, Sweden and eastern Canada. Large deformation finite element (FE) analyses were performed using the Coupled Eulerian-Lagrangian (CEL) method in Abaqus, which allows for capturing of the full progressive failure mechanism (initiation, propagation and breakoff) involved in a sensitive clay slide. The 1984 slide in Vestfossen, Norway, was chosen as problem case of progressive failure in sensitive clay to be back-calculated by using the CEL FE-model. It is found that the failure mechanism predicted by the FE-analysis agrees reasonably well with the historical failure mode observed at Vestfossen. A parametric study has been performed on the remoulded shear strength as well as the rate of strain softening of the sensitive clay in order to evaluate their effects on the landslide run-out distance.

31.1 Introduction

Most natural sensitive clays exhibit strain-softening behaviour which is generally a governing material property for progressive failure mechanisms. It is especially important for Scandinavian sensitive clays, which under large strains turns into a liquid with almost zero remoulded shear strength (Thakur and Degago 2012). Due to the progressive type of failure, a small local bearing capacity type of instability may potentially become a failure threshold triggering large devastating slides. The failure

P. Fornes (✉)
Norwegian Geotechnical Institute (NGI), Oslo, Norway

Norwegian University of Science and Technology (NTNU), Trondheim, Norway
e-mail: pfo@ngi.no

H.D.V. Khoa
Norwegian Geotechnical Institute (NGI), Oslo, Norway

V. Thakur et al. (eds.), *Landslides in Sensitive Clays*, Advances in Natural and Technological Hazards Research 46, DOI 10.1007/978-3-319-56487-6_31

can occur quite rapidly, essentially in undrained conditions (Locat et al. 2013). This type of hazard can cause significant damage to infrastructure, like the collapse of the Skjeggestad bridge in Norway in 2015, and loss of life.

Numerous methods have been developed, however, not many are capable of predicting the complete process of progressive failure involving its initiation, propagation and breakoff in sensitive clays. The main objective of the present study is to perform large deformation analysis of undrained slope stability in sensitive clays by using the Coupled Eulerian-Lagrangian (CEL) method available in the commercial finite element (FE) program Abaqus (2014). Many researchers have demonstrated that the CEL method is suitable for solving slope stability problem involving large deformations (Wang et al. 2013; Dey et al. 2015; Trapper et al. 2015). In this paper the CEL method is applied to simulate both the landslide triggering threshold and the landslide run-out distance.

The paper is organized in three main parts. In the first part, the CEL method is briefly introduced and the problem case of the 1984 slide in Vestfossen, which was chosen for the FE back-analysis, is described. The second part of the paper is devoted to provide some details about the CEL FE-model of the Vestfossen slide, the material inputs to the FE-model as well as a parametric study of the effect of strain-softening rate on the run-out distance of the failure. Finally, in the third part, the calculated FE-results are discussed and some concluding remarks are drawn from the present study.

31.2 Method: CEL

To calculate the full progressive failure mechanism involved in a quick clay slide, a numerical method that can handle large deformations is essential. In the standard Lagrangian FE method, excessively distorted elements during large deformation analysis can introduce error into the analysis results, and, in the worst case, they can cause the analysis to terminate prematurely.

The Coupled Eulerian-Lagrangian method is available in the Abaqus/Explicit program (Abaqus 2014), in which the element mesh is fixed in space and does not change with time while the material points (Gauss points) can flow freely across the mesh. In a CEL FE-model, the Lagrangian body and Eulerian body are discretized differently in separate (or with some overlap) regions of the problem domain. The Eulerian material can interact with Lagrangian elements through Eulerian-Lagrangian contact formulated based on an enhanced immersed boundary method. In this method the Lagrangian structure occupies void regions inside the Eulerian mesh. The contact algorithm automatically computes and tracks the interface between the Lagrangian structure and the Eulerian materials. Hence, the CEL method is suited for numerical problems involving large deformations due to the fact that there is no distorted element as illustrated in Fig. 31.1. The CEL method has been successfully used to model backward progressive sensitive clay slides, capturing the characteristic horsts and grabens modes of deformation (Dey et al. 2013, 2015).

Fig. 31.1 Illustration of deformed mesh obtained from Lagrangian analysis and CEL analysis

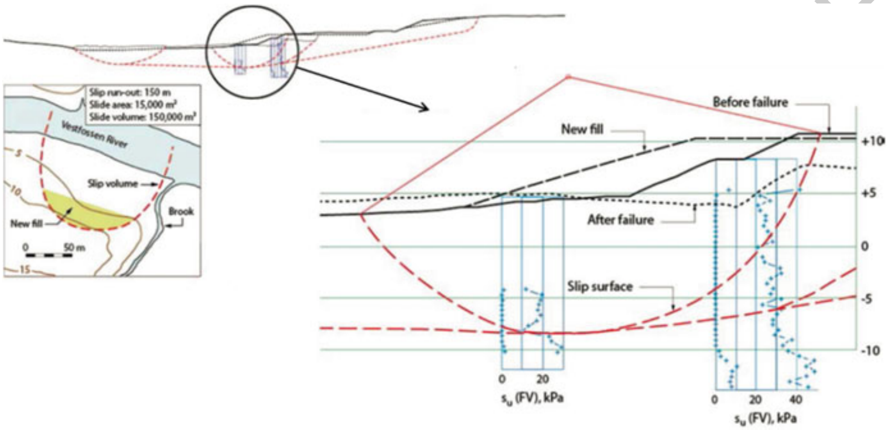

Fig. 31.2 Extent of the 1984 slide at Vestfossen (Modified from Kalsnes et al. 2013)

31.3 Problem Case: Vestfossen

The 1984 slide in Vestfossen, Norway, was chosen as problem case to investigate the effect of post peak stress strain behaviour on run-out distance of a quick clay landslide. The slide comprised an area of approximately 100 × 150 m, with roughly 10 m depth (Karlsrud 1984). The failure mechanism propagated horizontally quite far over a flat area, crossing the Vestfossen river, see Fig. 31.2.

The Vestfossen slide was most likely triggered by the construction of a new fill in a slope next to the Vestfossen river (NGI 1984), when a new soccer field was to be built. The very sensitive clay underneath the fill was thus mobilized past its peak undrained shear strength, which due to strain softening reduced the soil strength. This caused a downward progressive failure mechanism, where the local failure propagated almost horizontally over a larger distance. Soil investigations were performed after the slide, and the shearing plane was localized in the layer where the remoulded shear strength was close to zero in vane shear tests as shown in the cross section in Fig. 31.2.

The initiation of the slide was back calculated in a previous study (NGI 2012), using the (small strain) FE software Plaxis 2D (2015) with the user defined material

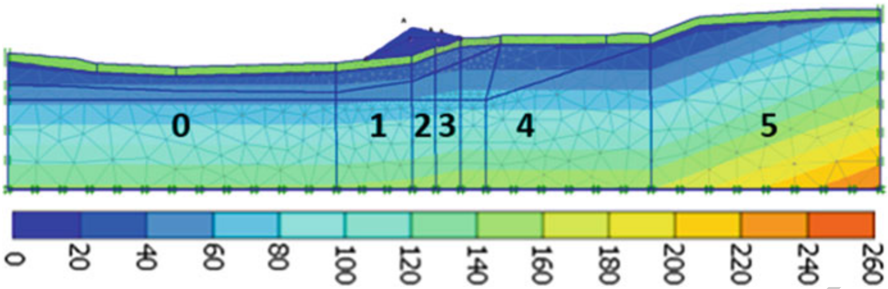

Fig. 31.3 Plaxis 2D model, undrained shear strength s_u^A [kPa] contours (Adapted from NGI 2012)

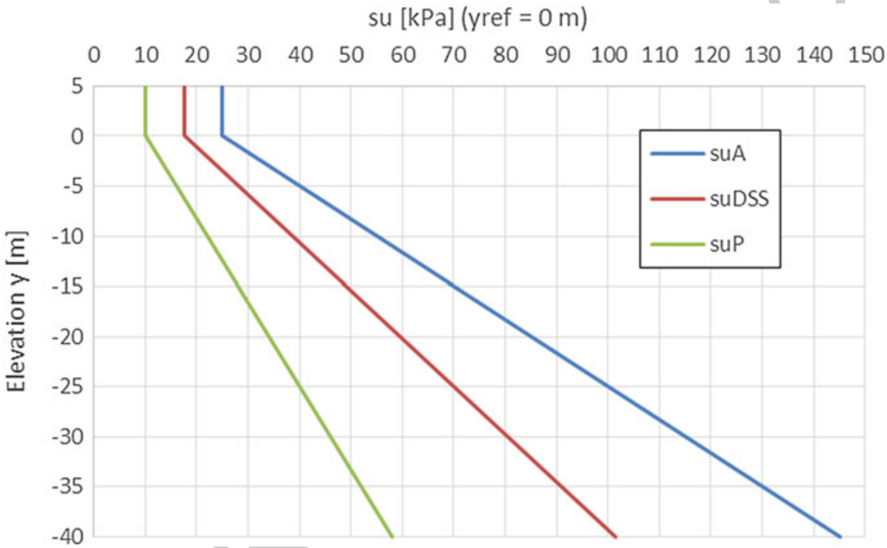

Fig. 31.4 Example of undrained shear strength profile, showing peak s_u values versus elevation in Section 0 ($y_{ref} = 0$ m). For isotropic strength, $s_u^{ave} = s_u^{DSS}$ was used

model NGI-ADPSoft, which could account for strain softening and anisotropy (Grimstad et al. 2010; Grimstad and Jostad 2010; Jostad and Grimstad 2011). The peak undrained shear strength profile was based on the available site data, and calibrated through back-calculation.

In a vertical cross section, the peak undrained shear strength increases linearly with depth from reference elevation y_{ref}. This parameter varies linearly in the horizontal direction within the sections 0–5 in Fig. 31.3, providing compatible strength contours for the different slope angles. The undrained shear strength profile is illustrated in Fig. 31.4, for Section 0 where the reference elevation $y_{ref} = 0$ m.

31.4 Abaqus CEL Modelling

In the current study, the Vestfossen cross section in Fig. 31.3 was modelled with Abaqus CEL as a 3D profile with 1 m unit thickness in the plane direction. The soil profile composed of a continuous layer of sensitive clay, with a dry crust material in the top 3 m and a fill that was applied to initiate failure. To apply the soil self-weight as the load gravity loading was used with acceleration 10 m/s^2 in negative y-direction (vertically) for simplicity. The respective unit densities then provides the volume mass. Each CEL FE-analysis is run as an explicit calculation, and a time interval for each calculation phase is given so that the velocities and kinetic energy become very small at the end of the phases. In the first phase the gravity was applied to the initial soil profile and the void, but not the fill, to provide the initial stresses. In the second phase, the gravity was also applied to the fill to initiate slope failure. In order to avoid unwanted numerical dynamic issues, the gravity loads were applied gradually over 10 seconds with the 'smooth step' function.

The CEL mesh size had (roughly) element size of 1 m, and thus only one element in the plane direction. The total number of elements was 22,755. A mesh sensitivity study was performed to see the effect of mesh fineness, where the length of the elements was reduced to 0.5 m. When using strain softening material behavior without any form of regularization, localization of shear bands and mesh size dependent results are expected. The user defined model in the small strain FE study (NGI 2012) used a non-local strain technique (Brinkgreve 1994), but the Mohr Coulomb material model in Abaqus does not include any regularization technique. However, the deformations with the finer mesh were comparable to the deformations with the original mesh. Hence, the original mesh was considered fine enough for this study.

31.4.1 Material Properties

31.4.1.1 Dry Crust

The 3 m dry crust in the top of the profile was described by the Mohr-Coulomb constitutive model with friction angle $\phi = 30°$, cohesion $c = 5$ kPa, Young's modulus $E = 10{,}000$ kPa, Poisson's ratio $\nu = 0.495$ and density $\rho = 1{,}800$ kg/m^3.

31.4.1.2 Fill Material

The fill behaviour was described by the Mohr-Coulomb material model with friction angle $\phi = 30°$, cohesion $c = 1$ kPa, Young's modulus $E = 10{,}000$ kPa and Poisson's ratio $\nu = 0.495$. The weight of the fill material was applied in the CEL calculations to initiate a local bearing capacity failure, and density $\rho = 1{,}800$–$2{,}000$ kg/m^3 was used. The necessary density depends on the degree of strain softening, and was initially determined from the Plaxis 2D FE-analysis.

31.4.1.3 Sensitive Clay Layers

The sensitive clays behaved undrained and were described by the Mohr-Coulomb constitutive model. For the elastic properties Young's modulus E = 30,000 kPa at elevation y_{ref} and increasing with depth 3,600 kPa/m, Poisson's ratio $\nu = 0.495$ and density $\rho = 1{,}800\ \mathrm{kg/m^3}$ were considered.

The standard Mohr Coulomb model in Abaqus was used to specify the variation of the cohesion (i.e. undrained shear strength) of the clays as a function of the plastic shear strain. For better comparison with possible future work, curve points of the cohesion and the corresponding plastic shear strain were specified so that the stress-strain softening curve has the same shape as in the NGI-ADPSoft model. The stress strain curves in the NGI-ADPSoft model are determined by the two state variables κ_1 and κ_2, respectively pre and post peak hardening functions. The functions are chosen so that the slope (first derivative) is zero at peak and residual strength

$$\kappa_1 = 2\cdot\left(\gamma^p/\gamma_p{}^p\right)^{0.5}/\left(1+\gamma^p/\gamma_p{}^p\right),\ \kappa_2 = \left(\left[\gamma^p - \gamma_p{}^p\right]/\left[\gamma_r{}^p - \gamma_p{}^p\right]\right)^{C1}\cdot\left(2 - \left[\gamma^p - \gamma_p{}^p\right]/\left[\gamma_r{}^p - \gamma_p{}^p\right]\right)^{C2}$$

where γ^p is the plastic shear strain, $\gamma_p{}^p$ is the peak strength plastic shear strain, $\gamma_r{}^p$ is the residual strength plastic shear strain, and $1.0 \le C2 \le C1 \le 2.0$ are constant to control the shape of the post peak softening curve. For this study the parameter set $C1 = C2 = 1.5$ was chosen.

In order to define increasing undrained shear strength with depth, the cohesion was given as a function of temperature. The temperature parameter was only used as a variable to provide different strength gradients corresponding with Fig. 31.3. Anisotropic strength and stiffness properties can be specified with the NGI-ADPSoft model, but isotropic is required with the Mohr Coulomb model in Abaqus. Thus, isotropic properties were used for this study, with peak undrained shear strength $s_{u,p} = s_u{}^{ave} = s_u{}^{DSS} = 0.7\cdot s_u{}^C$, according to Fig. 31.4.

Normalized residual undrained shear strength $s_{u,r}/s_{u,p} = 0.1$ was considered as the base case. The plastic shear strain at peak strength $\gamma_p{}^p = 3\%$ and the plastic shear strain at residual strength $\gamma_r{}^p = 30\%$ were used as the base case. The corresponding shear stress-strain curve is indicated with a black line in Fig. 31.5. To prevent the volume upslope from the fill from sliding out in the CEL calculation, the normalized residual strength $s_{u,r}/s_{u,p}$ in Section 4 and 5 of Fig. 31.3 was increased to 0.3 and 0.5, respectively.

31.4.2 *Parametric Study*

A parametric study was performed where the potential effect of strain-softening rate on the run-out distance was investigated. Only the properties of the sensitive clay layers downslope (in Section 0–3, Fig. 31.3) were varied. The normalized residual

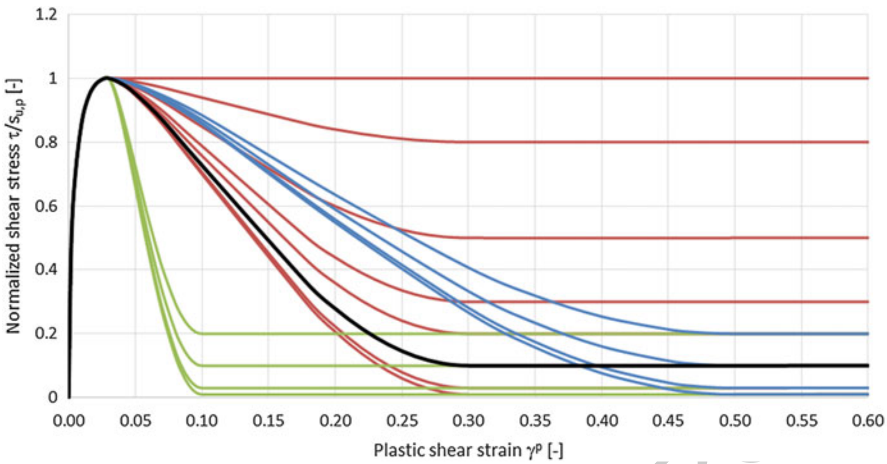

Fig. 31.5 Different normalized stress-strain curves considered in parametric study. *Black solid curve* corresponding to base case with $s_{u,r}/s_{u,p} = 0.1$, $\gamma_p{}^p = 3\%$, $\gamma_r{}^p = 30\%$

strength $s_{u,r}/s_{u,p}$ of these sensitive clay layers was varied between 0.01 and 1.0. The parameter controlling the rate of strain softening, the shear strain at residual strength $\gamma_r{}^p$, was varied from 10% to 50%. Note that a lower value of $\gamma_r{}^p$ results in a more brittle behavior. The stress-strain curves considered are illustrated in Fig. 31.5.

31.5 Results

The calculated results from the Abaqus CEL simulation of the base case strain-softening parameters are discussed here. The weight of the fill was applied from time T = 20 s to T = 30 s and the fill started to move after the full load had been applied. The only forces acting on the soil were the gravity and inertial loads. The kinetic energy of the whole system is a useful indicator to check if the soil failure mechanism has been stabilized. It can be seen in Fig. 31.6 that the kinetic energy increases as the local bearing capacity failure is initiated, and the peak kinetic energy appears at roughly T = 35 s. The motion slows down and the kinetic energy in the whole system is reduced to zero at roughly time T = 50 s.

The calculated average plastic shear strains and the velocity during the propagation of soil failures are illustrated in Fig. 31.7. The shading contours of plots with 5 s intervals are shown from time T = 30 s when the full fill weight has been applied to T = 50 s when the soil failure surface has stopped propagating.

A local failure is first initiated by the fill, and shear strains are developed in front of the slide as it is moving. The fill itself is not moving very far, but the downward progressive mechanism propagating is pushing material in front of the fill and is causing heave in the downstream area. After the main movement of the

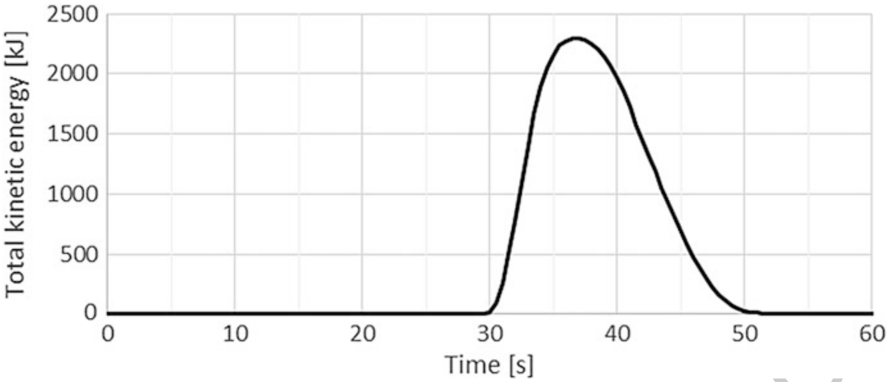

Fig. 31.6 Kinetic energy versus time. Peak when the slide is moving, goes down to zero

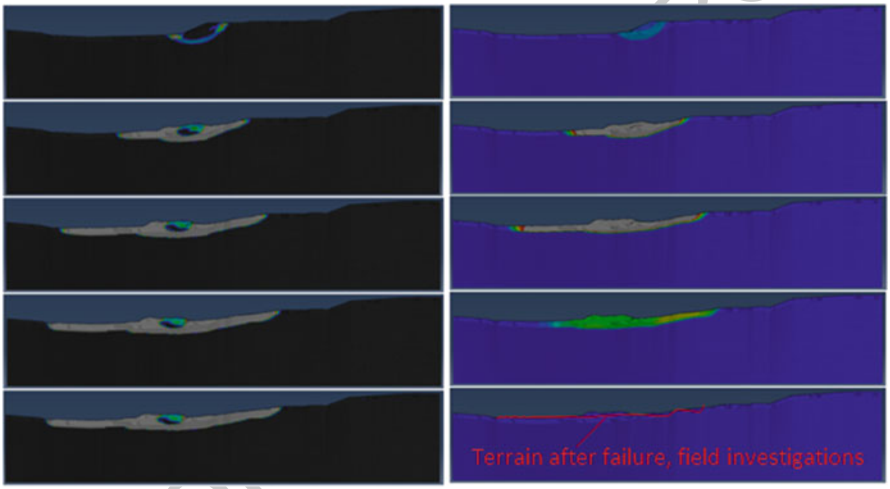

Fig. 31.7 Contours of (*left*) average plastic shear strain PEEQAVG (3–30%, i.e. peak to residual strength) and (*right*) velocity V (0–1 m/s) for time T = 30–50 s for the base case. The red line indicates the profile after failure that was recorded in the field investigation (Fig. 31.2)

fill, shear strains develop backwards, causing the slope to become gradually less inclined. It can be seen from the velocity contours that first the fill moves, followed by movement upslope after the fill volume has stopped.

31.5.1 *Comparison with Field Data*

The profile recorded in the field investigation after the Vestfossen landslide in 1984 is shown Fig. 31.2. The fill volume appears to have ended up completely flat horizontally, and one retrogressive failure surface appears behind the local fill failure surface. There was registered heave as far as 90 m from the toe of the fill, on the other side of the river.

The large deformation shape of the Abaqus CEL model calculation in Fig. 31.7 is comparable to the historical failure mode. In the calculations the fill volume is moving a distance from the toe and its contours remains in the terrain when the deformations stops. The terrain behind the fill also deforms, but not directly as a retrogressive failure surface. The authors believe that by refining the layer modelling to better match the in-situ conditions, a realistic upslope deformation pattern could be obtained, as demonstrated by Dey et al. (2015). The base case calculations include heave roughly 90 m from the toe of the fill, as observed.

The calculated deformation patterns seems to mainly take place in the top of the clay layers, right below the dry crust. In the historical slide, the propagating failure surface was most likely deeper indicated by in-situ vane shear tests. This could possibly be replicated by introducing anisotropy and constant residual strength with depth. The residual strength increased with depth since constant $s_{u,r}/s_{u,p}$ ratio and peak strength increasing with depth was used in the calculations. By introducing sensitive clay layers of different strengths instead of a homogenous layer, the CEL FE-analysis can provide better prediction of the identified failure surface.

31.5.2 Parametric Study

In the parametric study the effect of the post peak strength reduction curve parameters on the run-out distance was investigated. Due to the distinct mode of deformation, there is not a unique way to define the run-out distance. Two measures describing the run-out distance are reported; one is the extent of downstream heave due to the propagation of shear strains, distance measured from the toe of the applied fill, and the second is the crest movement of the fill.

The results from the parametric study are plotted in Fig. 31.8 showing run-out distance for different values of normalized residual undrained shear strength $s_{u,r}/s_{u,p}$ and the residual strength plastic shear strain $\gamma_r{}^p$. Due to model boundaries, 120 m was the maximum run-out distance.

31.6 Conclusions

The 1984 Vestfossen landslide has been back-analyzed using the CEL FE-model. It is found that the calculated failure pattern is in reasonable agreement with the historical failure mode observed at Vestfossen. A parametric study has been performed on the remoulded shear strength and the rate of strain softening of the sensitive clay in order to evaluate their effects on the landslide run-out distance. It appears that low residual strength values have a bigger effect than the degree of brittleness.

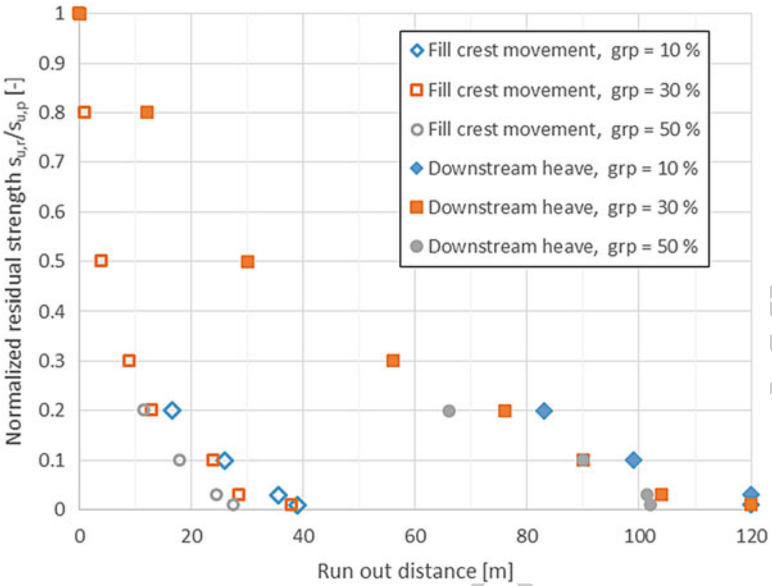

Fig. 31.8 Run-out distance (downstream heave and fill crest movement) versus normalized residual strength, with curves for different plastic shear strain at residual strength

Combining the CEL FE-model and an advanced constitutive model, which can account for the strain-softening behaviour and the anisotropic strengths in soils, provides a robust and suitable numerical tool for not only predicting landslide triggering threshold but also estimating landslide run-out distance in sensitive clays. However, applying different loads was not as easy as in a Lagrangian method due to the material deforming within the mesh, and the results can be mesh dependent due to no regularization with strain-softening.

Further work planned includes implementing the anisotropic NGI-ADPSoft model into the Abaqus/Explicit. This will enable the use of more realistic soil properties and better prediction of trigger load and run-out distance.

Acknowledgments The research has been supported by the Norwegian Geotechnical Institute. The authors also express their sincere thanks to Dr. Hans Petter Jostad for his assistance. Many thanks are given to Dr. Ha H. Bui for good feedback.

References

Abaqus (2014) Users' manual – version 6.14. Providence: Dassault Systems Simulia Corp., http://www.3ds.com/

Brinkgreve RBJ (1994) Geomaterial models and numerical analysis of softening. PhD thesis, TU Delft, Delft, The Netherlands

Dey R, Hawlader B, Phillips R, Soga K (2013) Progressive failure of slopes with sensitive clay layers. In: Proceedings of the 18th International Conference on Soil Mechanics and Geotechnical Engineering, Paris

Dey R, Hawlader B, Phillips R, Soga K (2015) Large deformation finite-element modelling of progressive failure leading to spread in sensitive clay slopes. Géotechnique 65(8):657–668. doi:10.1680/geot.14.P.193

Grimstad G, Jostad HP (2010) Undrained capacity analyses of sensitive clays using the nonlocal strain approach. In: 9th HSTAM International Congress on Mechanics Vardoulakis mini-symposia, Limassol, Cyprus

Grimstad G, Andresen L, Jostad HP (2010) NGI ADP: anisotropic shear strength model for clay. Int J Numer Anal Methods Geomech 36(4):483–497

Jostad HP, Grimstad G (2011) Comparison of distribution functions for the nonlocal strain approach. In: Proceedings of 2nd international symposium on computational geomechanics, Kroatia

Kalsnes BG, Gjelsvik V, Jostad HP, Lacasse S, Nadim F (2013) Risk assessment for quick clay slides – the Norwegian practice. In: 1st international workshop landslides in sensitive clays. Québec, Oct 2013

Karlsrud K (1984) Progressive failure in stiff overconsolidated and soft sensitive clays. Contribution to discussion session 9A – “Geologic aspects of slope stability problems”, ICSMFE

Locat A, Jostad HP, Leroueil S (2013) Numerical modeling of progressive failure and its implications for spreads in sensitive clays. Can Geotech J 50(9):961–978

NGI (1984) Strandajordet, Vestfossen, Utredning vedrørende utglidningen den 11. september 1984, samt de stabilitetsmessige konsekvenser for idrettsanlegget. NGI report 82032–3

NGI (2012) Effekt av progressiv bruddutvikling for utbygging i områder med kvikkleire, A2 Tilbakeregning av skred. NGI report 20092128-00-5-R, available as NIFS report 56/2014 at http://www.naturfare.no/_attachment/668507/binary/976962

Plaxis (2015) Plaxis 2D, www.plaxis.nl

Thakur V, Degago S (2012) Quickness of sensitive clays. Géotech Lett 2(3):87–95. doi:10.1680/geolett.12.0008

Trapper PA, Puzrin AM, Germanovich LN (2015) Effects of shear band propagation on early waves generated by initial breakoff of tsunamigenic landslides. Mar Geol 370:99–112

Wang D, Randolph MF, White DJ (2013) A dynamic large deformation finite element method based on mesh regeneration. Comput Geotech 54:192–201

AUTHOR QUERY

AQ1. Please provide mail id for the author 'Huynh D. V. Khoa'